MET.O.14

METEOROLOGICAL OFFICE
BOUNDARY LAYER RESEARCH BRANCH
TURBULENCE & DIFFUSION NOTE

T.D.N. No. 169

Application of the Jackson and Hunt Linear Analytical Model to Practical Wind-flow Problems

R H MARYON and MISS M L MACARI

March 1985

TDN 169

KW/33

Application of the Jackson and Hunt Linear Analytical Model to Practical Wind-flow Problems

R H MARYON and MISS M L MACARI

March 1985

Application of the Jackson and Hunt Linear Analytical Model to Practical Wind-flow Problems

Introduction

The first part of this paper gives an account of the Jackson and Hunt linear analytical theory of the wind component perturbations as air traverses a hill of slight to moderate slope. Topics covered are the original theory of Jackson and Hunt, the extension of the theory to 3-dimensional topography, and further refinements used in Met. Office versions. Of the latter, models C and D, due to P J Mason, are now programmed for routine application.

This account draws freely from:

Jackson and Hunt, 1975,	henceforth	JH
Mason and Sykes, 1979,	"	MS
Walmsley, Salmon & Taylor, 1982	"	WST
Taylor, Walmsley and Salmon, 1983	"	TWS
Mason and King, 1985	"	MK

It differs from JH in dealing with the 3-dimensional application and omitting the wealth of analytical detail in which the method of solution is embedded. From the other papers it differs in setting out, step by step, the full solution of the problem. A number of these papers contain comparisons with experimental results.

The second part of the paper describes the computer program, which can be adapted for application to specific wind-flow problems. The program can be used without familiarity with the underlying theory, but it is most important that users should keep in mind the limitations of the analysis, as detailed in part II, section 1.

PART I: THEORY

1. The solution of the 2-dimensional problem

1.1 Specifying the problem

JH contains the linear asymptotic theory of turbulent wind flow over a 2-dimensional hill of slight to moderate slope. They assumed a logarithmic upwind profile in a boundary layer of depth δ:

$$\left.\begin{aligned} u_o(z) &= \frac{u_*}{k} \log_e {}^{z}/_{z_o}, \qquad z < \delta \\ u_o &= \frac{u_*}{k} \log_e {}^{\delta}/_{z_o}, \qquad z \geq \delta \end{aligned}\right\} \quad (1)$$

Here, k is von Karman's constant, u_* the friction velocity, z the height above surface and z_o the roughness length. The flow, (fig. 1) is divided into an inner layer of depth l in which the turbulence adjusts rapidly to the increased shear, and an outer layer where the turbulence time scales are comparable with the time of transit over the hill, and the eddies are strained and distorted in broad accordance with rapid distortion theory (Britter et al 1981).

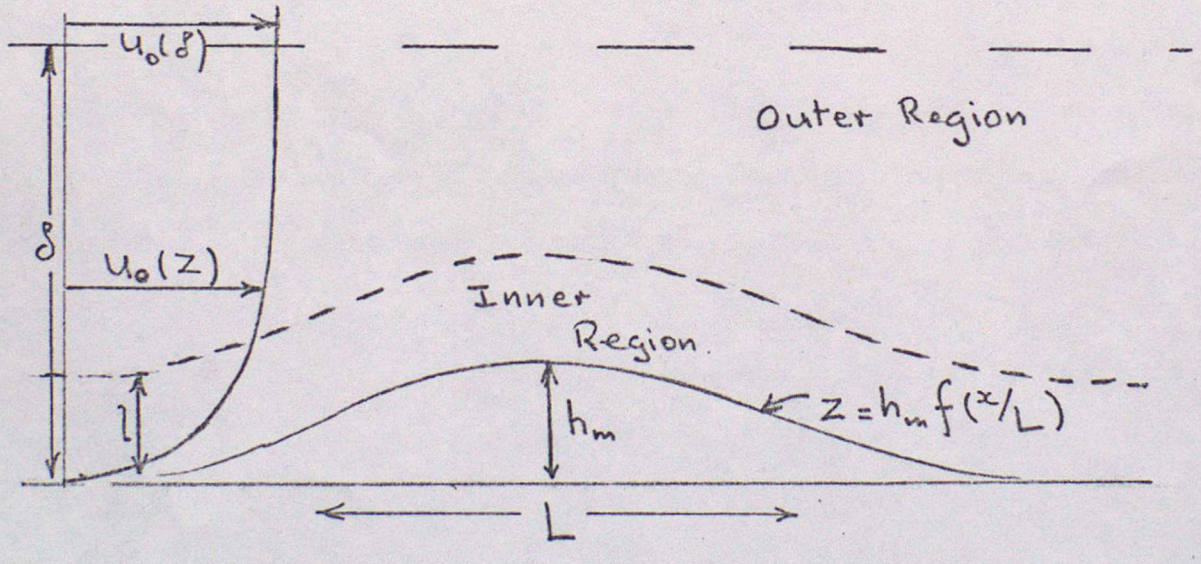

Fig. 1.

The length scale of the hill is L, the maximum height h_m, and non-dimensional coordinates X, Z are defined $X = {}^{x}/_{L}$, $Z = \dfrac{z - h_m f(X)}{l}$

where the hill profile is from $z = h(x/L) = h_m f(x/L)$. f is a smooth function such that the slope $h_m f'(x/L)/L < 1$. Z is the dimensionless distance above the surface.

JH assume that the streamwise velocity over the hill is

$$u(x,z) = u_0[z - h_m f(X)] + \varepsilon u_* U(X,Z) \qquad (2)$$

ie $u(x,z)$ is obtained from the upstream velocity profile at a similar height above the surface plus a small perturbation. U is a dimensionless perturbation velocity and $\varepsilon \ll 1$ a small parameter which provides a scale for the perturbation velocities. l was obtained by balancing the terrain-induced pressure gradient and stress gradient terms in the non-dimensional Navier-Stokes equation for the inner layer, and ε was obtained by the asymptotic matching of the inner and outer layer equations for the vertical component of velocity. In effect, the inner layer acceleration, pressure and stress gradient perturbations are balanced, the pressure being generated in the outer layer by the vertical displacement. The inner layer pressure perturbation matches that at the base of the outer layer. The analysis yields

$$(l/L)\log_e(l/z_0) = 2\kappa^2$$

or

$$l = 2L\kappa u_*/u_0(l) \qquad (3)$$

$$\varepsilon = \frac{h_m \log_e^2(L/z_0)}{L\kappa \log_e(l/z_0)} \qquad (4)$$

The non-dimensional forms for perturbation pressure, P, and surface stress, $\hat{\tau}_{xz}$, are from

$$\Delta\tau_{xz} \simeq \varepsilon\rho u_*^2 \hat{\tau}_{xz} \qquad (5)$$

$$\Delta p \simeq \frac{\varepsilon\rho u_*^2}{\kappa} \log_e(1/z_0) P(X,\zeta) \qquad (6)$$

where, for the outer layer, $\zeta = z/L$.

A first-order mixing length closure is used with the perturbation kinematic stress defined as the difference between the perturbed and undisturbed upstream values:

$$\Delta\tau_{xz} = \tau_{xz} - \rho u_*^2$$

Using (5) and a conventional mixing length (Prandtl) representation of surface stress the result

$$\hat{\tau}_{xz} = 2kZ\frac{\partial U}{\partial Z} \qquad (7)$$

is obtained and the linearised inner layer non-dimensional equation of motion reduces to

$$\frac{\partial U}{\partial X} = -\frac{\partial P_0}{\partial X} + \frac{\partial}{\partial Z}\left(Z\frac{\partial U}{\partial Z}\right) \qquad (8)$$

where $P_0 \equiv P(X,0)$. For the outer layer

$$\frac{\partial U}{\partial X} = -\frac{\partial P}{\partial X} \qquad (9a)$$

$$\frac{\partial W}{\partial X} = -\frac{\partial P}{\partial \varsigma} \qquad (9b)$$

where W is the perturbation vertical velocity.

1.2 Method of Solution

Using the equation of continuity (9a),(9b) yield

$$\nabla^2 P = 0 \qquad (10)$$

where $\nabla^2 = \frac{\partial^2}{\partial X^2} + \frac{\partial^2}{\partial \varsigma^2}$. By using the Fourier transform (Bracewell, 1965)

$$\tilde{P}(\alpha) = 4\int_{-\infty}^{\infty} P(X)\, e^{-2\pi i \alpha X}\, dX \qquad (11)$$

with the condition that $P \to 0$ as $X \to \pm\infty$ an equation with a single independent variable is obtained:

$$-\alpha^2 \tilde{P} + \frac{\partial^2 \tilde{P}}{\partial \varsigma^2} = 0$$

with a solution, for bounded $\tilde{P}$

$$\tilde{P}(\alpha) = A e^{-\alpha \varsigma} \qquad (12)$$

A can be obtained from the boundary conditions. MS point out that at the surface the dimensionless vertical velocity

$$W = \frac{\partial f}{\partial X}$$

so that using (9b)

$$\frac{\partial P}{\partial \zeta} = - \frac{\partial^2 f}{\partial X^2} \qquad (13)$$

ie.

$$\frac{\partial \tilde{P}}{\partial \zeta} = \alpha^2 \tilde{f} \qquad (14)$$

From (12) and the surface boundary condition (14)

$$\tilde{P}(\alpha) = - \alpha \tilde{f} e^{-\alpha \zeta} \qquad (15)$$

so that at the surface

$$\tilde{P}_o(\alpha) = - \alpha \tilde{f} \qquad (16)$$

It is now possible to solve the inner layer equation (8). Applying Fourier transforms similar to (11) yields

$$i\alpha \tilde{U}(\alpha) = - i\alpha \tilde{P}_o(\alpha) + \frac{\partial}{\partial Z} \left[Z \frac{\partial \tilde{U}(\alpha)}{\partial Z} \right] \qquad (17)$$

a differential equation which is transformable to a modified Bessel's equation of order zero. This is done by assuming that in the inner layer $\frac{\partial P}{\partial Z} \simeq \frac{\partial P_o}{\partial Z} = 0$ and making the substitution $Z' = 2(i\alpha Z)^{1/2}$

to obtain

$$z'^2 \frac{\partial^2(\tilde{u}+\tilde{P}_o)}{\partial z'^2} + z' \frac{\partial(\tilde{u}+\tilde{P}_o)}{\partial z'} - z'^2(\tilde{u}+\tilde{P}_o) = 0 \qquad (18)$$

The general solution is $AK_o(z') + BI_o(z')$ where K_o and I_o are the modified Bessel functions. For $\tilde{u}$ bounded as $z' \to \infty$ we obtain

$$\tilde{u} + \tilde{P}_o = AK_o(z')$$

From the boundary conditions $\tilde{u} = 0$ on $Z_o = z_o/l$ the inner layer solution

$$\tilde{u} = \tilde{P}_o \left[1 - \frac{K_o(2(i\alpha Z)^{1/2})}{K_o(2(i\alpha Z_o)^{1/2})} \right] \qquad (19)$$

is obtained. The inverse Fourier transform, e.g.

$$P_o(X) = \int_{-\infty}^{\infty} \tilde{P}_o(\alpha)\, e^{2\pi i \alpha X}\, d\alpha$$

requires integration over the wave numbers α to arrive at the solution - in practice the summation of a truncated series.

2. Extension to 3 dimensions

MS extended the JH theory to 3 dimensions, so that practical application could be made to real terrain. The hill profile now becomes

$\bar{z} = h_m f(x/L, y/L) = h_m f(X, Y)$. The steps of the analysis remain similar to JH, but now the pressure perturbation in the outer layer produces a gradient in the inner layer in the transverse, y, direction, of the same order as that in the x direction. Hence a perturbation velocity $\varepsilon u_* V(X, Y, Z)$ is induced and the inner layer equations

$$\frac{\partial U}{\partial X} = -\frac{\partial P_0}{\partial X} + \frac{\partial}{\partial Z}\left(Z \frac{\partial U}{\partial Z}\right) \qquad (20a)$$

$$\frac{\partial V}{\partial X} = -\frac{\partial P_0}{\partial Y} + \frac{1}{2}\frac{\partial}{\partial Z}\left(Z \frac{\partial V}{\partial Z}\right) \qquad (20b)$$

derived. As the equations are linearized the perturbation velocity V does not appear in the U equation. The factor 2 in (20b) is due to the consideration that the stress component τ_{xz} reflects perturbations in both the eddy viscosity and velocity gradient, while for τ_{yz} the perturbation velocity gradients have no effect on the eddy viscosity (to 1st order). The outer region equations are

$$\left.\begin{aligned} \frac{\partial U}{\partial X} &= -\frac{\partial P}{\partial X} \\ \frac{\partial V}{\partial X} &= -\frac{\partial P}{\partial Y} \\ \frac{\partial W}{\partial X} &= -\frac{\partial P}{\partial \zeta} \end{aligned}\right\} \qquad (21)$$

yielding $$\nabla^2 P = 0$$

where ∇^2 is now $\frac{\partial^2}{\partial X^2} + \frac{\partial^2}{\partial Y^2} + \frac{\partial^2}{\partial S^2}$.

The solution effectively follows the same steps as the 2-dimensional case, but now requires 2-dimensional Fourier transforms. As the details will be given for a similar calculation in the next section, it is only necessary here to quote the results:

$$\tilde{P}_o(k,m) = -\frac{k^2 \tilde{f}}{(k^2+m^2)^{1/2}} \qquad (22a)$$

$$\tilde{U}(k,m) = \frac{k^2 \tilde{f}}{(k^2+m^2)^{1/2}}\left[1 - \frac{K_0(2(ikZ)^{1/2})}{K_0(2(ikZ_0)^{1/2})}\right] \qquad (22b)$$

$$\tilde{V}(k,m) = \frac{km \tilde{f}}{(k^2+m^2)^{1/2}}\left[1 - \frac{K_0(2(2ikZ)^{1/2})}{K_0(2(2ikZ_0)^{1/2})}\right] \qquad (22c)$$

where k, m are wavenumbers in the x and y directions, requiring the inverse Fourier transform.

3. Later Developments: Model A

MK revert to the dimensional form of the equations of motion and carry out a standard linearization to obtain the perturbation equations

Outer layer:

$$u_0 \frac{\partial U}{\partial x} = - \frac{\partial P}{\partial x} \qquad (23a)$$

$$u_0 \frac{\partial V}{\partial x} = - \frac{\partial P}{\partial y} \qquad (23b)$$

$$u_0 \frac{\partial W}{\partial x} = - \frac{\partial P}{\partial Z} \qquad (23c)$$

Inner layer:

$$u_0 \frac{\partial U}{\partial x} = - \frac{\partial P_0}{\partial x} + \frac{\partial}{\partial Z}\left[2k(Z+z_0)u_* \frac{\partial U}{\partial Z}\right] \qquad (24a)$$

$$u_0 \frac{\partial V}{\partial x} = - \frac{\partial P_0}{\partial y} + \frac{\partial}{\partial Z}\left[k(Z+z_0)u_* \frac{\partial V}{\partial Z}\right] \qquad (24b)$$

where the closure is of a conventional mixing length form, u_0 a basic flow speed in the x direction, $Z = z - h(x,y)$ the height above surface, now defined by the height of the relief $h(x,y)$, and the perturbations $P = \Delta p/\rho$, where ρ is the air density, assumed constant. By scaling the inner layer vertical coordinate by $1/L$, i.e. using $z_s = Z/1/L$, with $z_{0,s} = z_0/1/L$, the inner layer equations are more conveniently written, using (3)

$$u_0 \frac{\partial U}{\partial x} = - \frac{\partial P_0}{\partial x} + \frac{\partial}{\partial z_s}\left[(z_s + z_{0,s})u_0 \frac{\partial U}{\partial z_s}\right] \qquad (25a)$$

$$u_0 \frac{\partial V}{\partial x} = - \frac{\partial P_0}{\partial y} + \frac{1}{2}\frac{\partial}{\partial z_s}\left[(z_s + z_{0,s})u_0 \frac{\partial V}{\partial z_s}\right] \qquad (25b)$$

(cf equations (20a), (20b)).

Using the continuity equations system (23) yields

$$\nabla^2 P = 0 \qquad (26)$$

The dimensional lower boundary condition is from $W = U_0 \frac{\partial h}{\partial x}$ on $Z = 0$.

Using (23c)

$$\frac{\partial P}{\partial Z} = -U_0^2 \frac{\partial^2 h}{\partial x^2} \qquad (27)$$

To solve (26) given (27), two-dimensional transform pairs are defined (as in WST) using truncated Fourier series to represent functions over the finite domain $X_0 \le x \le X_0 + L_1$, $Y_0 \le y \le Y_0 + L_2$. For example, for $h(x,y)$ we define

$$\tilde{h}(k',m') = \frac{1}{L_1 L_2} \int_{X_0}^{X_0+L_1} \int_{Y_0}^{Y_0+L_2} h(x,y) \cdot \exp\left[-2\pi i \left(\frac{k'x}{L_1} + \frac{m'y}{L_2}\right)\right] dy\, dx \qquad (28)$$

$$h(x,y) = \sum_{k'=-\infty}^{\infty} \sum_{m'=-\infty}^{\infty} \tilde{h}(k',m') \exp\left[2\pi i \left(\frac{k'x}{L_1} + \frac{m'y}{L_2}\right)\right] \qquad (29)$$

The transform (28) is, in practice, applied to a digitized topography using a fast Fourier transform computer package. For convenience, express the wavenumbers $k = \frac{2\pi k'}{L_1}$, $m = \frac{2\pi m'}{L_2}$, so that the exponential terms take the form (for example)

$$e^{-i(kx+my)}$$

Applying Fourier transforms to (26), (27) yields

$$-(k^2+m^2)\tilde{P} + \frac{\partial^2 \tilde{P}}{\partial Z^2} = 0 \qquad (30)$$

subject to the boundary condition at $Z = 0$

$$\frac{\partial \tilde{P}}{\partial Z} = u_0^2 k^2 \tilde{h} \qquad (31)$$

Given $\tilde{P} \to 0$ as $Z \to \infty$ (30) has the solution

$$\tilde{P} = Ae^{-(k^2+m^2)^{1/2} Z}$$

Applying (31) yields

$$\tilde{P} = -\frac{u_0^2 k^2 \tilde{h}}{(k^2+m^2)^{1/2}} e^{-(k^2+m^2)^{1/2} \cdot Z} \qquad (32)$$

So that at the surface

$$\tilde{P}_0 = -\frac{u_0^2 k^2 \tilde{h}}{(k^2+m^2)^{1/2}} \qquad (33)$$

As the inverse transform is expressed

$$P = \sum_{k=-\infty}^{\infty} \sum_{m=-\infty}^{\infty} \tilde{P}\, e^{-i(kx+my)}$$

substitution from (32) gives

$$P = \sum_{k=-\infty}^{\infty} \sum_{m=-\infty}^{\infty} \frac{-u_o^2 k^2 \tilde{h}}{(k^2+m^2)^{1/2}} \cdot e^{-(k^2+m^2)^{1/2} Z} \cdot e^{-i(kx+my)}$$

and writing $n = i(k^2+m^2)^{1/2}$ yields

$$P = \sum_{k=-\infty}^{\infty} \sum_{m=-\infty}^{\infty} \tilde{P}_o\, e^{i(kx+my+nZ)} \qquad (34)$$

Result (33) permits the solution for the inner layer. Fourier transform of (25a), for example, gives

$$ik(u_o \tilde{U} + \tilde{P}_o) = \frac{d}{dz_s}\left[(z_s + z_{o,s})\, u_o \frac{d\tilde{U}}{dz_s}\right]$$

which on substitution of $\xi = 2(ikz_s)^{1/2}$ (cf (22b), (22c)) and recalling $\frac{\partial \tilde{P}}{\partial \xi} = 0$ yields (except for heights very close to z_o)

$$\xi^2 \frac{\partial^2 (u_o \tilde{U} + \tilde{P}_o)}{\partial \xi^2} + \xi \frac{\partial (u_o \tilde{U} + \tilde{P}_o)}{\partial \xi} - \xi^2 (u_o \tilde{U} + \tilde{P}_o) = 0$$

a modified Bessel equation of zero order in $(u_o \tilde{U} + \tilde{P}_o)$. The solution follows similar lines to (19) and is usually expressed

$$\tilde{u} = -\frac{\tilde{P}_o}{u_o}\left[1 - \frac{K_o(2(iz')^{1/2})}{K_o(2(iz_o')^{1/2})}\right] \qquad (35a)$$

For the V component the Bessel equation is in $(ku_o\tilde{V} + m\tilde{P}_o)$, giving

$$\tilde{V} = -\frac{m\tilde{P}_o}{k u_o}\left[1 - \frac{K_o(2(2iz')^{1/2})}{K_o(2(2iz_o')^{1/2})}\right] \qquad (35b)$$

(compare system (22))

where $z' = kz_s = \frac{kZ}{l/L} = \frac{ku_oZ}{2ku_*}$; $z_o' = kz_{o,s} = \frac{kz_o}{l/L} = \frac{ku_oz_o}{2ku_*}$.

This is Model A of MK, and requires the inverse transform (29) for final solution. In practice this is done by fast Fourier transform.

4. Model C

The choice of a single-valued u_o as an advection velocity in a region where there is considerable vertical shear is arbitrary and may detract from the validity of the solution. Also, as pointed out in WST, equation (22a) can be approximated, over a range of k,m, by $\tilde{P}_o = -|k|\tilde{f}$ so that there is a substantial high wavenumber contribution to the pressure field. In practice the high wavenumber components of $\tilde{f}$ or $\tilde{h}$ are not known, or distorted by interpolation and digitization, so that they add noise to the solution.

The first refinement in MK (and adopted independently by TWS) is to choose outer layer velocity scales $u_s(k,m)$ at the wave scale heights $z_w = (k^2+m^2)^{-1/2}$. In effect advection velocities are adapted to the scales of the relief as interpreted in Fourier transform space. The same scales are used for the inner layer. The arguments of the Bessel functions in (35a), (35b) are accordingly replaced by

$$z' = \frac{ku_sZ}{2ku_*}, \quad z_o' = \frac{ku_sz_o}{2ku_*} \qquad (36)$$

and $u_s(k,m)$ substituted for u_o in (33), (35a), (35b).

Secondly, the inner and outer layer solutions are combined to allow the outer layer exponential decay of the perturbations with height to influence the inner layer. It is clear from (23a) that as U and P tend to zero as $x \to \infty$ the outer layer solution for the x-component is

$$U = P/u_o \qquad (37)$$

As $z' \to 0$ the outer layer solution (37) tends to $U = P_o/u_o$. Likewise, as $z' \to \infty$, the inner layer solutions (35a), (35b) tend to P_o/u_o. Accordingly, incorporating (36),

$$\tilde{P} = -\frac{u_s^2 k^2 \tilde{h}}{(k^2+m^2)^{1/2}} \cdot e^{-(k^2+m^2)^{1/2} \cdot Z} \qquad (38a)$$

$$\tilde{U} = -\frac{\tilde{P}}{u_s}\left[1 - \frac{K_o(2(iz')^{1/2})}{K_o(2(iz'_o)^{1/2})}\right] \qquad (38b)$$

$$\tilde{V} = -\frac{m\tilde{P}}{k u_s}\left[1 - \frac{K_o(2(2iz')^{1/2})}{K_o(2(2iz'_o)^{1/2})}\right] \qquad (38c)$$

is a universally valid solution combining the inner layer solution with the outer layer exponential decay with height: the effect of high wavenumber noise is reduced as Z increases.

5. Model D

The Model C solutions were found to give insufficient perturbation, and have not really solved the problem of the inner layer wind velocity scale which, for given (k,m), is fixed. Nor is it obvious what U,V are

perturbations from. MK point out that high in the inner layer a balance between the advection and the outer layer pressure field is approached; nearer the surface, in the 'equilibrium' region of shear-generated turbulence, a velocity scale based upon the height scale of the stres divergence is more appropriate. For Model D a velocity scale u_z is chosen which is equal to the upstream velocity at the height above the surface for which a flow prediction is required. The outer layer scale remains $u_s(h,m)$ as in model C. The solutions then become (38a) with

$$\tilde{u} = -\frac{\tilde{P}}{u_z}\left[1 - \frac{K_0(2(iz')^{1/2})}{K_0(2(iz'_0)^{1/2})}\right] \qquad (39a)$$

$$\tilde{v} = -\frac{m\tilde{P}}{k u_z}\left[1 - \frac{K_0(2(2iz')^{1/2})}{K_0(2(2iz'_0)^{1/2})}\right] \qquad (39b)$$

(where $z' = \frac{k u_z Z}{2K u_*}$, $z'_0 = \frac{k u_z z_0}{2K u_*}$), requiring inverse transforms in the usual way.

In the computer program all winds are scaled by an upstream 'geostrophic' value at height z_g so that $u(z_g) = 1$ and $u(z < z_g) < 1$. U and V are perturbations of u_z and are plotted in the model output (default option SCLP = UOUT) in the normalised form u/u_z, v/u_z so that the magnitudes of the perturbations for any specified, unscaled wind at height Z can be inferred immediately.

PART II: THE COMPUTER PROGRAM

1. Under the assumed conditions of a logarithmic wind profile with neutral static stability the drag coefficient

$$C_d = \left(K / \log_e Z/z_o \right)^2$$

so that with the winds scaled to unit velocity at the top of the mixed layer the perturbations depend solely upon the surface roughness. In the computer program provision exists for prescribing either a geostrophic drag coefficient or the roughness length. Models C and D are both available for practical application on a single computer program, for which a digitized topography must be supplied. It is most important that the user familiarize himself at the outset with the limitations of these models.

(1) The theory is a linear one, and can be applied only to relatively gentle slopes. Steep slopes and bluffs are often associated with powerful accelerations, flow-separation phenomena, wakes, etc which are outside the scope of the theory. In addition sharp corners or angles are difficult to represent using finite Fourier series.

(2) A uniform surface roughness is assumed, which may be inappropriate in reality, particularly where there are strong contrasts, such as a wooded island in a large lake, etc.

(3) The static stability of the air is neutral. The model is particularly inappropriate for stable conditions when, depending on the Froude number, the flow may follow the contours rather than accelerate up slope.

(4) The mixing length closure of the equations of motion is well known to have theoretical inadequacies.

(5) The upstream vertical wind profile is assumed logarithmic.

(6) The topography must be considered as isolated in a flat domain, as the theory requires all perturbations to be zero sufficiently far upstream and downstream. In other words the solutions using Fourier transforms require a periodic domain (in both x and y directions) and all perturbations must be contained within one wavelength.

2. Data Input and Adjustment of wind direction (program TROTATE)

The Jackson-Hunt model calculates perturbations to the mean wind over a prescribed orography of slight or moderate slope. In the Jackson-Hunt program the wind direction is always from the left hand side of the frame so first it may be necessary to rotate the 'hill'. This is effected using the program 'TROTATE', so that the wind approaches from the desired bearing. If no rotating is required the orography can be read straight from the data set by the Jackson Hunt program.

The hill or orography over which the airflow is required should be contour digitised and is read from device FTØ9 into array X (dimension 63 x 63). The mean altitude of the terrain surrounding the digitised orography should be determined and entered later via variable BASE in TJHUNT (section 3). The grid-length used in the digitisation must be used to compute the overall dimension of the domain used in the main program (127 grid-lengths for MX=MY=7, see section 3) and BX, BY in TJHUNT adjusted accordingly.

Array H contains the hill after rotation. THETA is the anti-clockwise angle of rotation, in degrees, (format F6.1) and array N provides different options for output (format 4I2), where N(I)=1 means option is required;

ie. if N(1)=1 array X is printed out in tables;

if N(2)=1 array H is printed out in tables;

if N(3)=1 array X is plotted using calcomp,

if N(4)=1 array H is plotted using calcomp,

Program Description

In the program, the coordinates of the grid are rotated clockwise using the transformation:-

X' = X cos(THETA) + Y sin(THETA)

and Y' = -X sin(THETA) + Y cos(THETA)

Subroutine HEIGHT computes the clockwise rotated grid-point heights by interpolation between the adjacent unrotated grid-points using:- $H' = \sum_{i=1}^{4} a_i h_i$

where $a_i = c_i \Big/ \sum_{j=1}^{4} c_j$ and $c_i = (p_1^2 + p_2^2)^{-1/2}$

(h_i are heights at the 4 adjacent gridpoints, p_1 and p_2 are the perpendicular distances from the rotated gridpoint to the appropriate row/column of the old grid).

These heights are then transferred to array H and inserted at the pre-rotation locations. THis has the effect of rotating the hill by THETA degrees anti-clockwise (N.B. an anticlockwise hill rotation through THETA degrees is equivalent to a clockwise rotation of wind direction through THETA-90 degrees in the output of the main Jackson-Hunt program; if THETA-90 degrees is negative the wind bearing is THETA+270 degrees).

The array containing the rotated hill is stored in a dataset on disk where it can be accessed by the Jackson-Hunt program.

The JCL to run 'TROTATE' is shown in Appendix A and sample calcomp output is shown in figure A(1).

3. Running the Jackson-Hunt Program TJHUNT

Input Data

The dataset containing the contour digitised array is read from FT09 by subroutine FILLUP, and is put into a larger array F, so that the hill should take up approximately 1/3 x 1/3 of the domain if it is comfortably contained in array H.

The input parameters are:-

TITLE ('A' format with a maximum of 36 characters).

&CNTL (namelist with choice of values as shown)&end

&PARMS (namelist with default values as shown) &END

NMAST (format I2)

(TMAST(I),DMAST(I),I=1,NMAST)-fortran 77 list format

THØ,TH1 (format 2F12,4).

TITLE:- A title can be read in if required; it will be printed in the heading of the contour map of the orography. If no title is required, leave a blank line.

&CNTL:- In this namelist the choice of model C or model D is controlled by the variable MODEL and the choice of specifying either a geostrophic drag coefficient DRAG or the (uniform) surface roughness length ZRØ is controlled by the variable INST. (It is not necessary to specify a wind strength or direction). Variable SCALE is used to scale the perturbations either with respect to the upstream wind at the same height or the unit upstream wind at the 'geostrophic' height ZUØ. The latter option allows perturbations at different levels to be compared directly.

Thus:- INST='DRSP' = > DRAG is specified (ZRØ is calculated).

INST='ZRSP' = > ZRØ is specified (DRAG is calculated).

MODEL='MODC' = > model C is required.

MODEL='MODD' = › model D is required.

SCLP='UOUT' => perturbations scaled by upstream wind at same height.

SCLP='UZUØ' => perturbations proportional to unit wind at height ZUØ.

defaults are INST='ZRSP'. MODEL'MODD' and SCLP='UOUT'

&PARMS has default values:-

MX=7 (2**MX is the number of grid points in the X-direction)

MY=7 (2**MY " " " " " " " " Y-direction)

The dimensions (number of grid-points) of the domain or of arrays H, X in TROTATE can be adjusted, if necessary by application to Met O 14. MX=MY=7 is appropriate for H(63,63) and yields F(128X128). Note that the dimension parameter IP depends upon MX, MY.

BX=5000. (box size in X-direction, in metres)

BY=5000. (" " " Y-direction, in metres)

BASE=0. (mean height of terrain surrounding hill, in metres)

ZROUT=10. (height (metres) at which flow is required)

ZUØ=1000. (height (metres) at which the scaled upstream velocity is unity).

DRAG=1.207 e-3 (drag coefficient)

ZRØ=0.01 (roughness length, in metres)

It is only necessary to overwrite ZRØ or DRAG depending upon the option INST.

ZUØ and DRAG define UØ the scaled logarithmic velocity profile eg.

UØ(ZUØ)=1.0

UØ(ZROUT)=(DRAG**0.5)/0.4*ALOG(ZROUT/ZRØ)

N.B. UØ≤1.0

NMAST is the number of 'masts' (maximum 15) for which a windstrength and angle are required. The strength is relative to unit or upstream value per option SCLP.

TMAST and DMAST are the coordinates for each mast; TMAST being the anti clockwise angle between north, the centre of the digitised orography (typically a hill-top), and the mast, DMAST being the distance in metres between the mast and the orography centre.

THØ (degrees) is the anticlockwise hill rotation (i.e. THØ=THETA). TH1 (degrees) is the anticlockwise angle from north defining a cross section of U and V from the hilltop perpendicularly to the edge of the frame. Thus a cross-section is only drawn if the angle between the cross-section and the wind bearing (section 2) is an integer multiple of 90 degrees.

4. Description of Output

Output is directed to film (FTØ8FØØ1) and paper (FTØ6FØØ1) the film output is a series of calcomp plots showing the following:-

(1) A contour map of the hill

(2) and (3) contour maps of the alongwind and crosswind (u and v) perturbation to the mean wind caused by the orography. Solid contours are positive, pecked contours negative. For the v perturbation positive is a deflection to the left looking downwind. Thus at height ZROUT (for SCLP option UOUT) if the mean wind upstream is 10 m/s, a 0.1 contour would represent a perturbation of 1 m/s. For SCLP option UZUØ all perturbations are fractions of the 'unit' geostrophic wind, but can be compared directly with the scaled upstream mean wind at the same height above surface, ZROUT, which is listed in the printed output.

(4) (optional) a graph showing a cross-section of velocity perturbations.

(5) A graph showing wind arrows over the whole domain.

The printed output includes:

Input data, maximum height of orography, upstream wind at height ZROUT and upstream friction velocity (U*) both scaled by wind strength at height ZUØ, maximum perturbation velocities and for each mast, u and v perturbations to the mean wind and the resultant strength and deflection.

The JCL to run 'TJHUNT' is shown in Appendix B and sample calcomp output is shown in Figure B(1).

Acknowledgement is due to Ms H.M. Schrecker, who carried out a substantial part of the computer programming in the early stages.

References

Bracewell, R. (1965)

The Fourier transform and its applications.

McGraw-Hill p.14.

Jackson, P.S. and Hunt, J.C.R. (1975)

Turbulent wind flow over a low hill.

Quart. J. R. Met. Soc. 101 pp929-955.

Mason, P.J., and King, J. (1985)

Measurements and predictions of flow and turbulence over an isolated hill of moderate slope.

To appear in April edition of Quart. J.R. Met Soc.

Mason, P.J. and Sykes, R.I. (1979)

Flow over an isolated hill of moderate slope.

Quart. J.R.Met. Soc. 105 pp 383-395.

Taylor, P.A., Walmsley, J.L., and Salmon, J.R., (1983)

A simple model of neutrally stratified boundary layer flow over real terrain incorporating wavenumber dependent scaling.

Boundary Layer Met. 26 pp169-189.

Walmsley, J.L., Salmon, J.R., and Taylor, P.A. (1982)

On the application of a model of boundary layer flow over low hills to real terrain.

Boundary Layer Met. 23 pp17-46.

```
//T14TTRTH JOB (M14,TT,P213),MACARI.2457,NOTIFY=T14TT,PRTY=??,TIME=(,10)
//*INFORM PRINTDATA
// EXEC FORTVCLG
//FORT.SYSIN DD DSN=M14.TLIB.FORT(TROTATE),DISP=SHR
//LKED.PLOT DD DSN=MET.CALCOMP,DISP=SHR
//LKED.CMAP DD DSN=M12.EA0B2,DISP=SHR
//LKED.FPNO DD DSN=M21.OBJLIB,DISP=SHR
//LKED.SYSIN DD *
  INCLUDE PLOT(CALCOMP,DASHP,RECT)
  INCLUDE CMAP(CMAPCALC,CMAPOUTP,CMAPLABS)
  INCLUDE FPNO(JIFPNO)
//GO.SYSIN DD *
 255.0 0 0 1 1
/*
//GO.FT01F001 DD SYSOUT=M,DCB=(RECFM=FBA,LRECL=133,BLKSIZE=1330)
//GO.FT07F001 DD SYSOUT=A,DCB=(RECFM=FBA,LRECL=133,BLKSIZE=1330)
//GO.FT08F001 DD SYSOUT=G,DCB=(RECFM=FB,LRECL=80,BLKSIZE=1680)
//GO.FT09F001 DD DSN=M14.TNYLAND.ARRAY,DISP=OLD,SPACE=(TRK,(1,1),RLSE)
//GO.FT10F001 DD DSN=M14.TROT.DATA,DISP=OLD
//
```

APPENDIX A: JOB CONTROL & SAMPLE INPUT FOR PROGRAM TROTATE.

ORIGINAL HILL

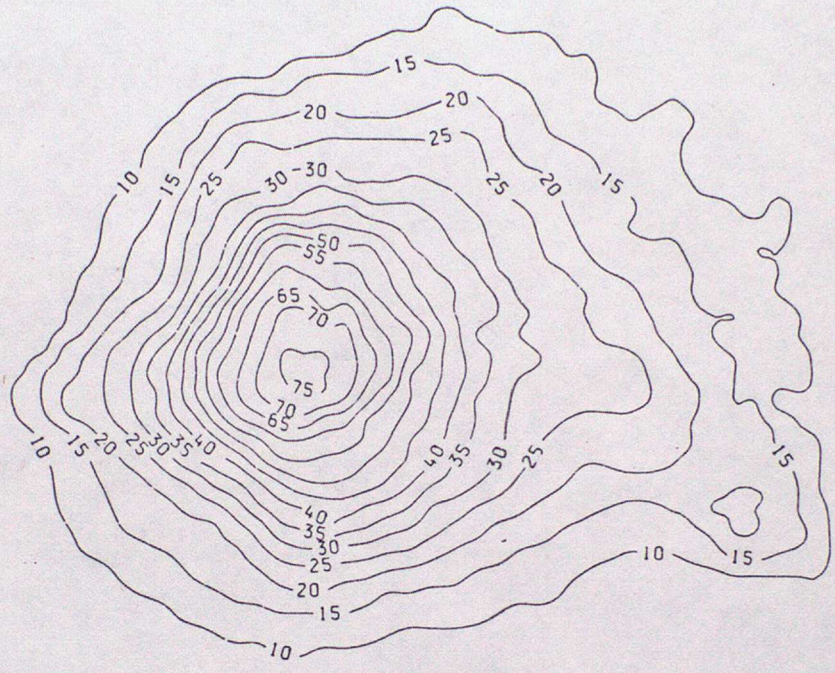

Fig. A(1a)

HILL AFTER ROTATION OF 2.55×10^{2} DEGREES

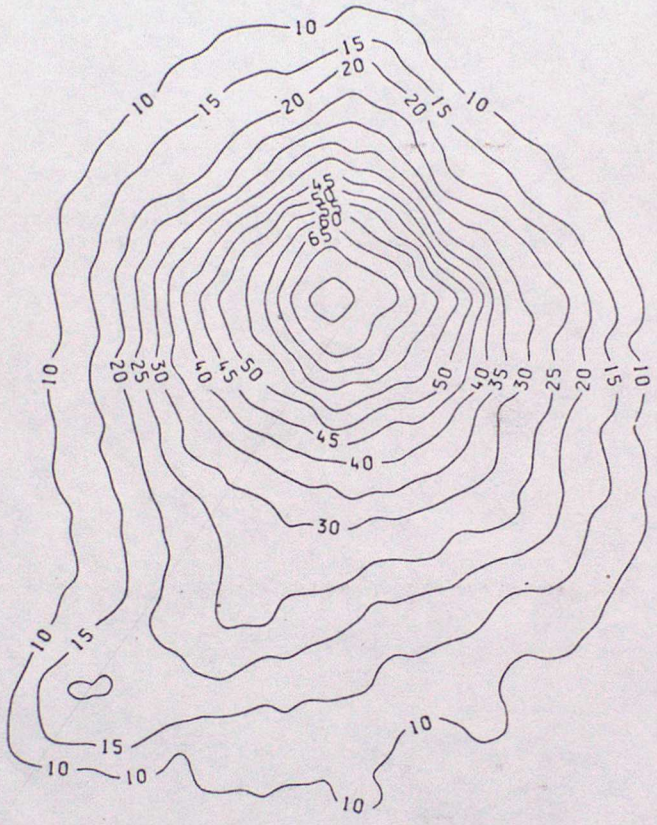

Fig. A(1b)

```
//T14TCSTC JCB (M14,TT,P213),MACARI.2457,NCTIFY=T14TT,PRTY=??,TIME=2
//*INFORM PRINTDATA
// EXEC FORTVCLG,FVREGN=1200K,R=T3
//FORT.SYSIN DD DSN=M14.SCURCE(HARM),DISP=SHR
// DD DSN=M14.TLIB.FORT(TJHUNT),DISP=SHR
//LKED.CALCOMP DD DSN=MET.CALCOMP,DISP=SHR
//LKED.JCNTR DD DSN=M21.OBJLIB,DISP=SHR
//LKED.SYSIN DD *
   INCLUDE CALCOMP(CALCOMP,ARCHC,AXIS,LINE,SCALE)
   INCLUDE JCNTR(JCNTR,JIFFNO)
/*
//GO.FT05F001 DD *
 NYLAND HILL
 &PARMS
 MX=7,MY=7,BX=2240.,BY=2240.,BASE=7.,ZRCUT=8.,ZLO=1000.,DRAG=1.207E-3
 ZRO=0.01
 &END
 &CNTL
 INST='ZRSP'
 MODEL='MODD'
 SCLF='UZUO'
 &END
15
80.0,125.0,100.0,125.0,120.0,125.0,140.0,125.0,160.0,125.0
180.0,125.0,200.0,125.0,220.0,125.0,240.0,125.0,260.0,125.0
178.5,108.3,205.0,121.4,181.0,198.0,194.0,209.2,187.0,203.6
0000255.0000000285.0000
/*
//GO.FT08F001 DD SYSOUT=G,DCB=(RECFM=FB,LRECL=80,BLKSIZE=1680)
//GO.FT09F001 DD DSN=M14.TRCT.DATA,DISP=OLD
//
```

APPENDIX B: JOB CONTROL & SAMPLE INPUT FOR PROGRAM TJHUNT.

INPUT TOPOGRAPHY FOR JACKSON-HUNT MODEL - NYLAND HILL

HILL AFTER ROTATION OF 2.55×10² DEGREES

CONTOUR INTERVAL= 5.00×10⁰ METRES

WIND DIRECTION= 1.65×10² DEGREES

Z-FIELD

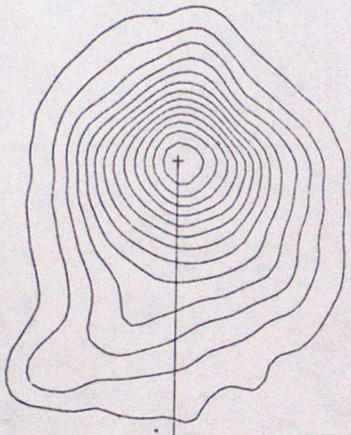

Fig. B(1a)

JACKSON-HUNT TURBULENT FLOW OVER 3-D HILL - MODEL D

PERTURBATIONS SCALED WITH RESPECT TO UNIT WIND AT ZUO IE. 1.00×10^{3} METRES

BOX DIMENSIONS 2.24×10^{3} X 2.24×10^{3}

UP WIND VELOCITY (AT HEIGHT ZROUT)= 5.81×10^{-1}

U-FIELD CONTOUR INTERVAL = 3.91×10^{-2}

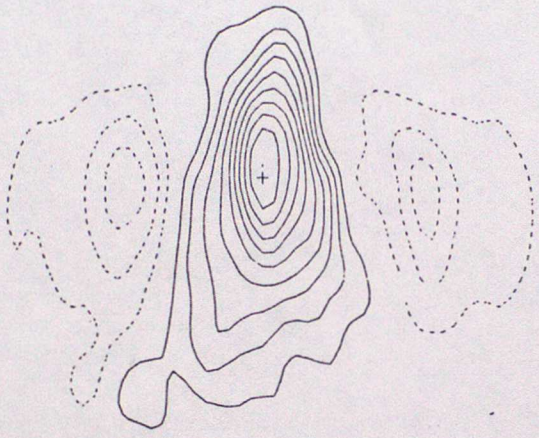

Fig. B(1b)

V-FIELD CONTOUR INTERVAL = 1.24×10^{-2}

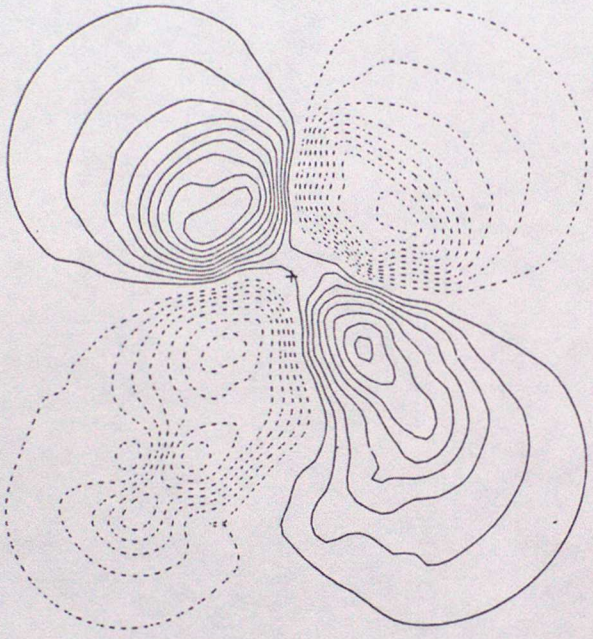

Fig. B(1c)

MAST TO HILL-TOP CROSS-SECTION 2.85×10² DEGREES ANTI-CLOCKWISE FROM NORTH

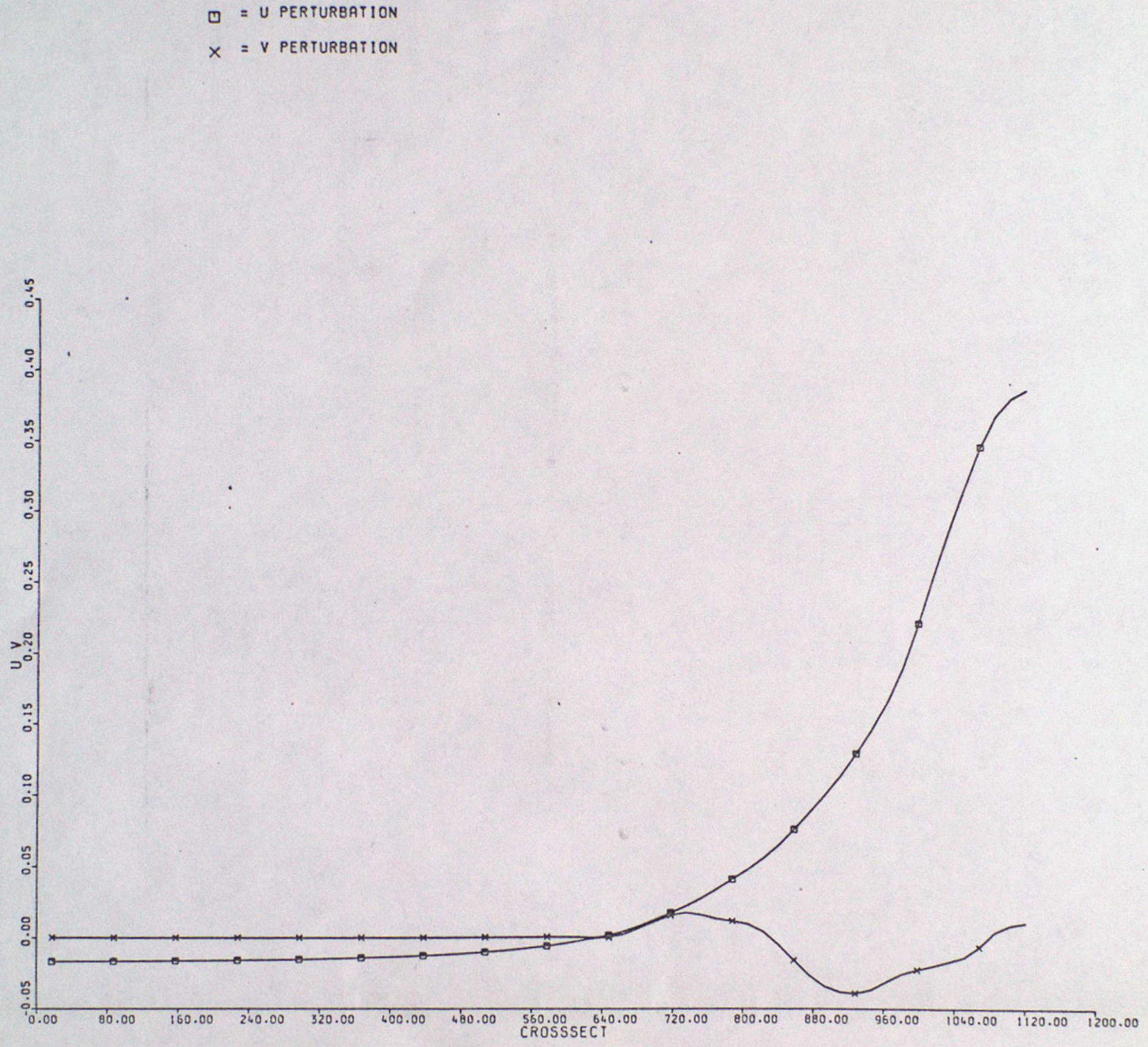

Fig. B(1d)

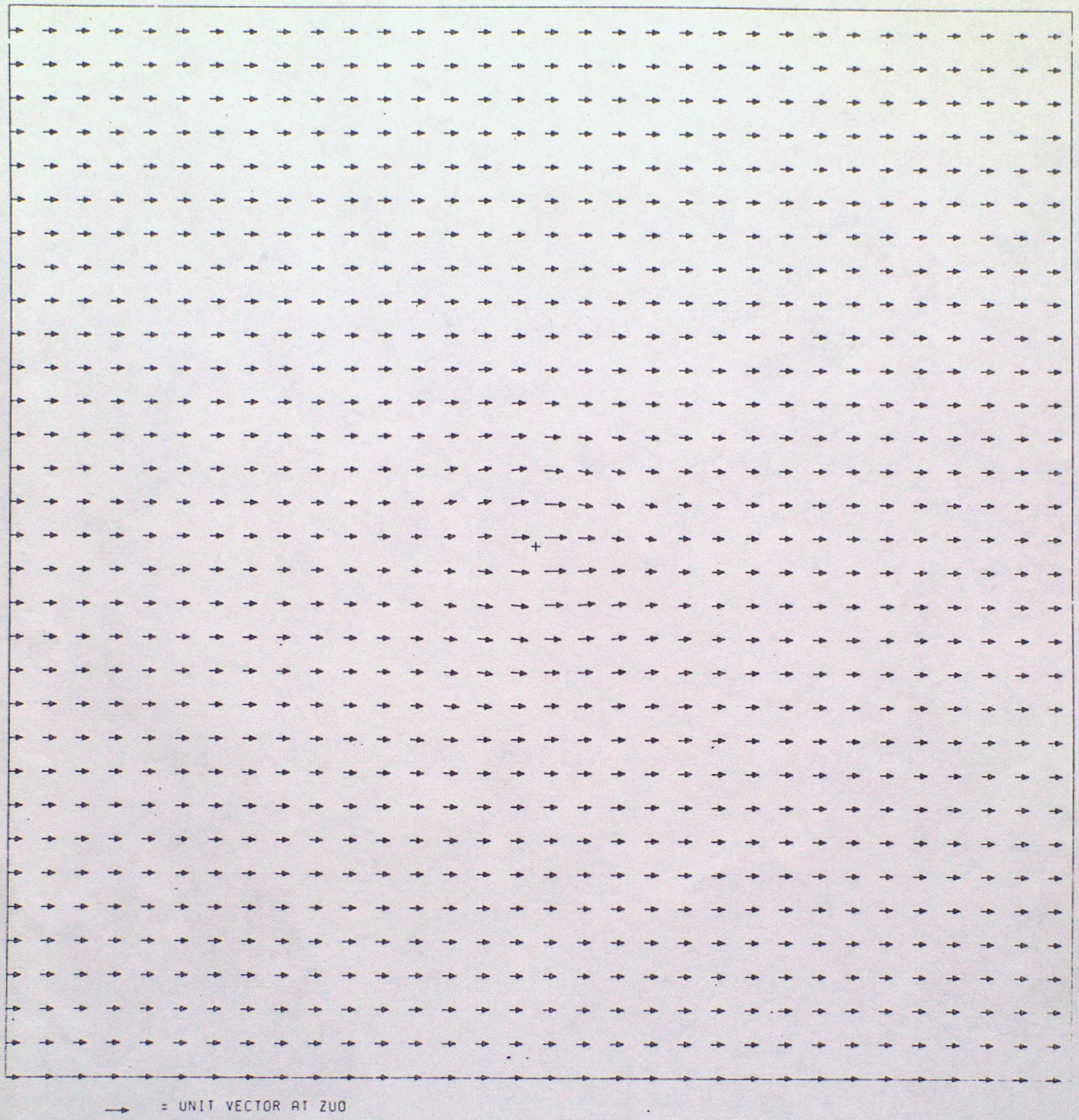

Fig. B(1e)